Asian Journal of Chemistry; Vol. 30, No. 8 (2018), 1711-1716

ASIAN JOURNAL OF CHEMISTRY

https://doi.org/10.14233/ajchem.2018.21245

# Study on Poly(vinyl alcohol) Coated Superparamagnetic Nanoparticles *via* RAFT Polymerization Methodology for Drug Delivery System Loaded Anti-Inflammatory

TRINH DUY NGUYEN[1], SANG THANH VO[1], VAN THI THANH HO[2], XUAN TIEN LE[3] and LONG GIANG BACH[1,*]

[1]NTT Institute of High Technology, Nguyen Tat Thanh University, 300A Nguyen Tat Thanh, District 4, Ho Chi Minh City, Vietnam
[2]Hochiminh University of Natural Resources and Environment, 236B Le Van Sy, Ward 1, Tan Binh District, Ho Chi Minh City, Vietnam
[3]Department of Chemical Engineering, HCMC University of Technology, VNU-HCM, 268 Ly Thuong Kiet Street, District 10, Ho Chi Minh City, Vietnam

*Corresponding author: Fax: +84 28 39404759; Tel: +84 96 9294297; E-mail: blgiang@ntt.edu.vn

*Received*: 21 January 2018; *Accepted*: 26 February 2018; *Published online*: 30 June 2018; AJC-18961

In this study, $Fe_3O_4$ magnetic nanoparticles grafted with poly(vinyl alcohol) (PVA-*g*-MNPs) were successfully fabricated *via* reversible addition-fragmentation chain transfer (RAFT) polymerization with two main steps: (a) chain transfer agent for RAFT, S-benzyl S′-trimethoxysilylpropyltrithiocarbonate was immobilized onto the surface of MNPs, and (b) poly(vinyl alcohol) was grafted onto the MNPs surface through RAFT polymerization. The results demonstrated the growth of PVA chains onto the surface of MNPs *via* directly hydrolyzed of PVA-*g*-MNPs. The covalent functionalization, structure, morphology and magnetic property of PVA-*g*-MNPs nanocomposites were characterized using XPS, FT-IR, EDX, TGA and SQUID analyses. In addition, drug loading/release potentialities of PVA-*g*-MNPs was investigated using ibuprofen as a model drug and evaluated using UV-visible spectroscopic technique. Evaluation of nano-medicine based on as-synthesized PVA-*g*-MNPs (*in vitro*) suggested that this material can be an attractive candidate for chemotherapeutic efficacy against cancer cell lines.

**Keywords: Poly(vinyl alcohol), Superparamagnetic nanoparticles, Drug delivery system, Cytotoxicity.**

## INTRODUCTION

Recently, considerable efforts have been dedicated to the creation and manipulation of materials at the nanoscale due to their novel properties and potential applications for biotechnology and life sciences [1-3]. Among these nanosystems, the design of organic-inorganic hybrid materials constructed by the combination of magnetic moieties and polymer matrices have been received much attention in biomedical applications, such as magnetic drug targeting, enzyme immobilization and hyperthermia anticancer strategy [4-6]. The rapid progression of polymer science and technology has well indicated that a vast array of organic-inorganic hybrid materials with desired properties, including electroactive, mechanical and thermal properties should be easily fabricated. There are numerous publications related to magnetic nanocomposite materials with the combination of different polymers and $Fe_3O_4$ magnetic colloids have been recently explored [7-11]. Recently, hydrophilic polymer polyvinyl alcohol (PVA) has been employed as a significant building block in biomedical and biotechnological applications due to its water solubility, biocompatibility and biodegradability [12-14]. In addition, commercially available PVA, which is prepared by the hydrolysis of poly(vinyl acetate), is known as the largest volume water-soluble polymer [15,16].

Many studies have been focused on the design of novel macromolecular constructions with well-defined structure over the past decades for both biotechnology and nanotechnology applications because this router is so versatile and can apply for the synthesis of the large range of functional polymers [17-19]. Moreover, with versatility and convenience of the free-radical process, the living/controlled free radical polymerization techniques have been extensively utilized for the fabrication of polymers. Especially, reversible addition-fragmentation transfer (RAFT) has the most attention in polymer technology, which can be employed for the preparation of commercially available polymers. This polymerization can operate with wide varieties of vinyl monomers without using metal catalysts under the mild conditions. Other benefits of RAFT polymerization is that this polymerization can be compatible with various monomers (including functional monomers), products have desired grafting density and narrow molecular weight distribution and this process can be performed in large range of reaction media, such as aqueous solutions, organic solutions, suspensions, emulsions and ionic liquids [20,21]. More recently, RAFT has been successfully

synthesized smart and hybrid materials by grafting polymer chains onto organic and/or inorganic surfaces [22-24].

Ibuprofen has been utilized as a medication in the non-steroidal anti-inflammatory drug (NSAID) class because of its strong anti-inflammatory, analgesic, antipyretic action and acceptable toxicity. In addition, with short biological half-life and good pharmacological activity, ibuprofen has been commonly used as a model drug for sustained and controlled drug delivery system [25-27]. To enhance biopharmaceutical properties of the drug, complexes and conjugates containing ibuprofen with high molecular weight compounds or nanosystems containing ibuprofen has been recently developed [28-32]. Herein, we present the synthesis of ibuprofen conjugates PVA-grafted $Fe_3O_4$ magnetic nanoparticles (PVA-*g*-MNPs), an antiproliferative activity against colorectal cancer cells *in vitro*. PVA-*g*-MNPs were prepared by RAFT polymerization with two main steps. The chain transfer agent for RAFT, S-benzyl S′-trimethoxysilylpropyl-trithiocarbonate, was first immobilized onto the surface of MNPs. Subsequently, poly(vinyl alcohol) was grafted onto the MNPs surface through RAFT polymerization and then its hydrolysis. The magnetic carriers were loaded with ibuprofen and its *in vitro* release profiles were investigated. *In vitro* studies of the ibuprofenconjugates, PVA-g-MNPs nanocarriers against A549 and EA.hy926 cancer cell lines proposed a remarkable promise for biomedical applications.

## EXPERIMENTAL

Vinyl acetate was removed the inhibitor before use by using $CaH_2$ and then being distilled under $N_2$ gas flow. 2,2′-Azobisisobutyronitrile (AIBN) was recrystallized from methanol solvent prior to use. Ferric chloride hexahydrate ($FeCl_3·6H_2O$), ferrous chloride tetrahydrate ($FeCl_2·4H_2O$), aqueous ammonia, sodium methoxide, carbon disulfide, benzyl bromide, 3-(mercaptopropyl)trimethoxysilane (MPTMS), *n*-propylamine, sodium hydroxide, ibuprofen, dimethyl sulfoxide and other solvents were of analytical grade (Sigma-Aldrich) and used without further purification.

FT-IR spectra were recorded on a BOMEM Hartman & Braun FT-IR Spectrometer. Field Emission Scanning Electron Microscopy (FE-SEM) and Energy Dispersive X-Ray (EDX) images were collected on a HitachiJEOL-JSM-6700F system, Japan. Thermogravimetric analysis (TGA) was carried out on a Perkin-Elmer Pyris 1 analyzer (USA). X-ray Photoelectron spectroscopy (XPS) were acquired on a Thermo VG Multilab 2000 in an ultra-high vacuum with Al Kα radiation. The magnetic properties were performed using a superconducting quantum interference device magnetometer (SQUID) (Quantum design MPMS-XL7, USA) at 300 K.

**Preparation of S′-(3-trimethoxysilyl)propyl trithiocarbonate (BTPT):** S′-(3-trimethoxysilyl)propyl trithiocarbonate (BTPT) were prepared according to the known procedure [33]. Briefly, sodium methoxide (0.81 g) in anhydrous methanol (5 mL) mixed to (3-mercaptopropyl)trimethoxysilane (MPTMS) (3.10 g) in anhydrous methanol (25 mL) under nitrogen with magnetic stirring. After 1 h, carbon disulfide (1.5 g) was added to the above solution and stirred for 5 h at room temperature. Subsequently, benzyl bromide (2.62 g) was added with continuous stirring overnight under nitrogen. Finally, orange oil (BTPT) was obtained by diluting with dichloromethane, filtering off and concentrated under reduced pressure until constant weight was achieved.

**Preparation of magnetic nanoparticles (MNPs):** Firstly, $FeCl_2·4H_2O$ (0.15 mol) and $FeCl_3·6H_2O$ (0.3 mol) were dissolved in aqueous medium (30 mL). Secondly, the pH of the mixed solution was adjusted to 13 using 0.4 M NaOH solution and stirred for 3 h under $N_2$ atmosphere. Finally, black precipitates of iron oxide was rinsed with distilled water several times and dried under vacuum at 40 ºC for 24 h.

**Immobilization of RAFT agent on magnetic nanoparticles (MNPs) surface:** Magnetic nanoparticles (MNPs) (0.2 g) and BTPT (0.5 g) were added to methanol (20 mL) with the help of ultrasound for 45 min. The mixed solution was then sealed under nitrogen and stirred overnight at ambient temperature. The obtained suspension was centrifuged at 9000 rpm for 30 min and the particles at bottom of the tube was washed with excess THF, followed by drying under vacuum at room temperature over night.

**Synthesis of PVA-*g*-MNPs by RAFT polymerization:** MNPs-RAFT (0.2 g), poly(vinly acetate) (2.15 g) and AIBN (8.2 mg) were added dropwise to methanol (4.0 mL). The mixture was degassed using three freeze-pump-thaw methods, sealed under nitrogen and subsequently heated at 60 ºC. Then, the mixed suspension was dissolved in tetrahydrofuran and precipitated in petroleum ether. Finally, obtained red-brown PVA-*g*-MNPs nanocomposites were dried in a vacuum oven at 40 ºC for 24 h.

**Hydrolysis of PVA-*g*-MNPs to get PVA-*g*-MNPs:** A mixture of *n*-propylamine (2.5 mL), PVA-*g*-MNPs (0.5 g), and methanol (10 mL) was continuously stirred for 30 min. Then, sodium hydroxide (0.5 g) in methanol (5 mL) was added to the above mixture with stirring for 12 h and keeping at room temperature. PVA-*g*-MNPs was separated with the assistant of a permanent magnet and washed with deionized water many times, followed by drying in the vacuum oven at 40 ºC for 24 h.

**Preparation of ibuprofen drug loading and release from PVA-*g*-MNPs system:** The PVA-*g*-MNPs sample (0.4 g) and ibuprofen (60 mg/mL) were added into hexane (50 mL) with stirring for 24 h in a sealed vial. The ibuprofen loaded PVA-*g*-MNPs sample (PVA-g-MNPs-ibuprofen) were then magnetically separated and dried at 45 ºC for 24 h. The release process of ibuprofen was given as follow: PVA-*g*-MNPs-ibuprofen (0.2 g) was immersed in the release media of simulated body fluid (SBF) and slow stirred at 37 ºC. The ratio of SBF/adsorbed ibuprofen was set at 1 mL/mg. At regular time intervals, the concentration of ibuprofen released was determined by UV-visible spectrophotometer at λ = 220 nm. Note that the ionic composition SBF solution and human body plasma were the same with a molar ionic composition of 142.0/5.0/2.5/1.5/147.8/4.2/1.0/0.5 for $Na^+/K^+/Ca^{2+}/Mg^{2+}/Cl^-/HCO_3^-/HPO_4^{2-}/SO_4^{2-}$ (pH = 7.4) [34].

**Evaluation of cytotoxicity of MNPs nanohybrids:** Cell culture and *in vitro* cytotoxicity assay of MNPs nanohybrids using an MTT (3-(4,5-bimethylthiazol-2-yl)-2,5-diphenyltetrazolium bromide, a tetrazole) assay. Human alveolar basal epithelial cells (A549 cells, American Type of Culture Collection, Manassas, VA, USA) and the human umbilical vein cell line

(EA.hy926, American Type of Culture Collection, Manassas, VA) were cultured in Dulbecco's Modified Eagle Medium (DMEM) supplemented with 10 % heat-inactivated fetal bovine serum (FBS), 2 mM l-glutamine, 10 mM 4-(2-hydroxyethyl)-1-piperazine ethanesulfonic acid (HEPES) buffer, 100 U/mL of penicillin G and 100 mg/mL of streptomycin. The cells were grown under a humidified atmosphere containing 5 % $CO_2$, at 37 ºC and in 96-well plates at a density of $2 \times 10^5$ cells/mL for 24 h. Then, cells were exposed to the samples with different concentrations and incubated in the above grown medium for 48 h. After the exposure to the samples, cells were washed and treated with 1 mg/mL of MTT solution for 4 h. Finally, after the supernatant was removed, 150 µL of DMSO was added to solubilize the formed formazan salt. The concentration of formazan salt was estimated by measuring the absorbance at 540 nm using a microplate reader (GENios® Tecan Austria GmbH, Austria). The cell cytotoxic level was calculated as a percentage compared to blank (without the addition of the samples).

## RESULTS AND DISCUSSION

**Structure analysis of PVA-*g*-MNPs nanocomposites: Scheme-I** displays the approach designed for the synthesis of reactive and magnetic nanocomposites, PVA-*g*-MNPs *via* RAFT polymerization.

In this work, MNPs were synthesized by co-precipitation method using $FeCl_3 \cdot 6H_2O$ and $FeCl_2 \cdot 4H_2O$ as $Fe^{3+}$ and $Fe^{2+}$ precursors ($Fe^{2+}/Fe^{3+}$ = 1/2 (mol/mol)), respectively. The as-synthesized MNPs were analyzed by FT-IR spectroscopic in the wave range of 4000-400 $cm^{-1}$ (Fig. 1A). As shown in Fig. 1A, strong vibrational bands around 3412 and 584 $cm^{-1}$ can be attributed to the stretching vibration of -OH groups on MNPs and Fe-O bond of bulk magnetic, respectively. The FT-IR spectrum of MNPs-RAFT sample (Fig. 1B) displayed absorption peaks ascribed to trithiocarbonate at 3440 $cm^{-1}$ and C-H stretching vibration of propyl group at 2926 $cm^{-1}$, implying the introduction of RAFT agent to the surface of MNPs. As also shown in Fig. 1B, absorption peaks ascribed to Fe-O-Si bond between MNPs and BTPT at 1126 $cm^{-1}$ and the characteristic absorption peak of Si-O-Si bond at 1034 $cm^{-1}$ indicated that silane groups undergo a self-condensation reaction to form a polysiloxane film on the MNPs surface. Fig. 1C displayed the FT-IR spectrum of

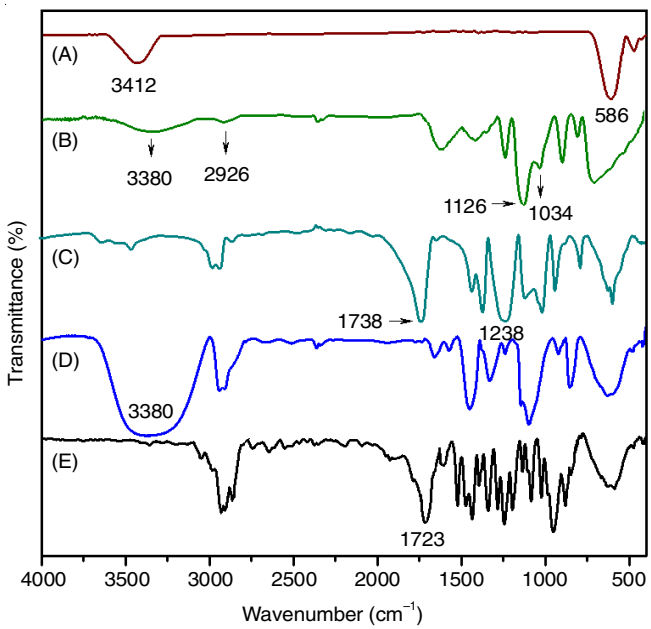


Fig. 1. FT-IR spectra of (A) MNPs, (B) MNPs-RAFT, (C) PVA-g-MNPsc, (D) PVA-g-MNPs and (E) PVA-g-MNPs-IBU

PVA-*g*-MNPs, the peak ascribed to C=O stretching at 1738 $cm^{-1}$ and C-O stretching at 1238 $cm^{-1}$, which confirmed the attachment of the polymer to MNPs. The C=O and C-O vibrations, which were the characteristic absorptions of PVAc, appeared and disappeared around 3380 $cm^{-1}$ is due to the contribution of hydrogen bond and hydroxyl groups of PVA. These results confirmed the successful hydrolysis of PVA-*g*-MNPs precursor in an alkaline medium to form PVA-*g*-MNPs and indicated that PVA was grafted on the surface of MNPs.

The surface chemical composition of RAFT agent immobilized and polymer coated MNPs were carried out by XPS and EDX analysis. Fig. 2A shows the broad scan XPS spectrum of MNPs, which is dominated by signals attributable to Fe, O and C elements. As shown in Fig. 2A, the binding energies of Fe2p (710.2 eV), O1s (530.8 eV) and C1s (285.1 eV) were obtained for the MNPs. This result is in concordance with the EDX results (Fig. 2D) which also suggested the presence of Fe, O and C elements in MNPs. The XPS spectra of each element of MNPs-RAFT are shown in Fig. 2B. The binding energies of

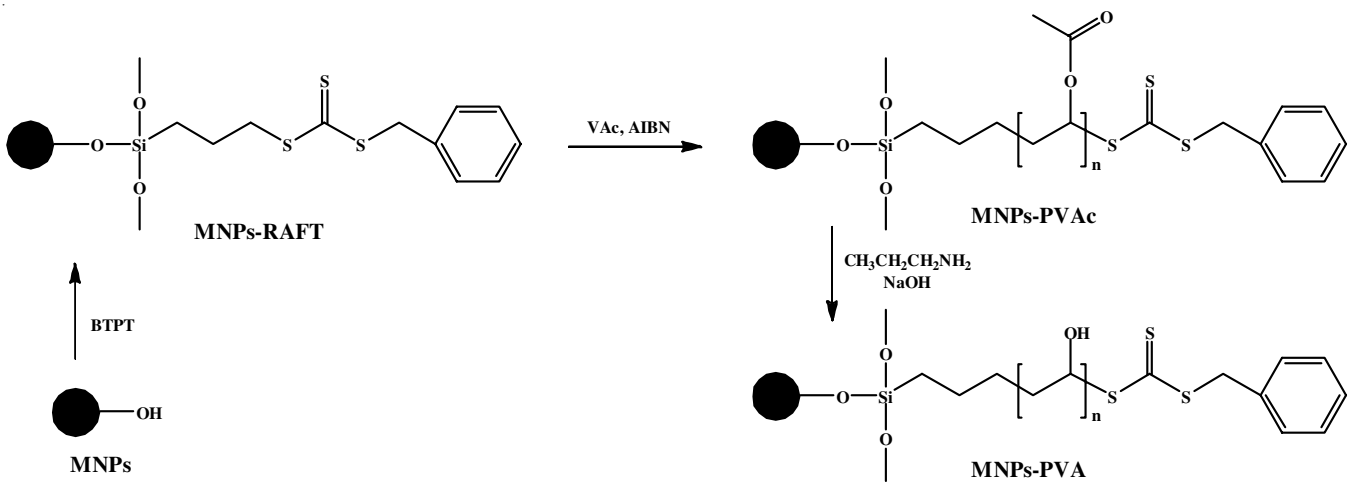


**Scheme-I:** Procedures used in this study for the surface modification of MNPs

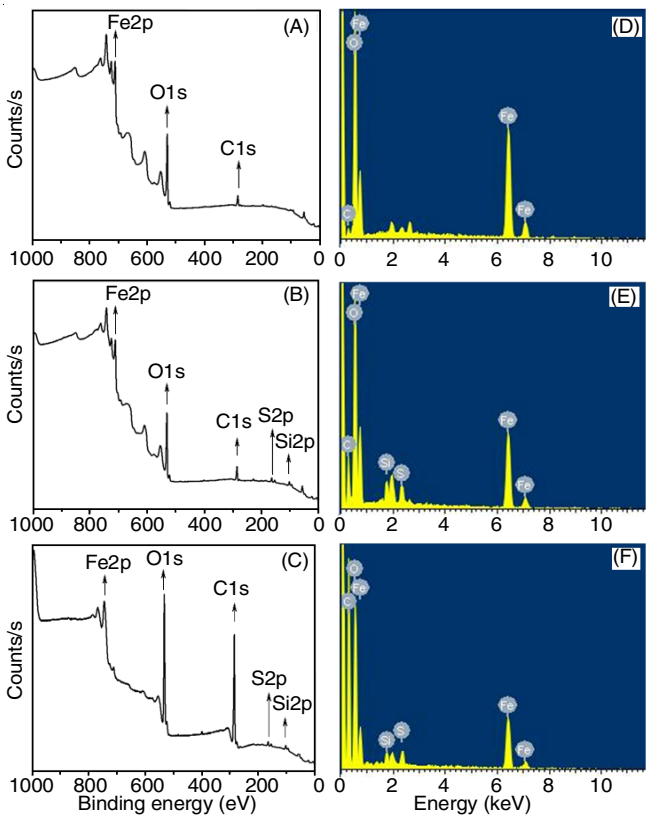


Fig. 2. XPS full-scan of (A) MNPs, (B) MNPs-RAFT, (C) PVA-g-MNPs; EDX spectrometric analysis of (D) MNPs, (E) MNPs-RAFT and (F) PVA-g-MNPs

Fe2p (710.5 eV), O1s (533.2 eV), C1s (284.8eV), Si2p (101.7 eV) and S2p (163.5 eV) were obtained for MNPs-RAFT, which confirms the presence of RAFT agent on MNPs surfaces. Fig. 2E presents EDX spectrum of MNPs-RAFT, which also confirmed the presence of RAFT agent on MNPs surfaces. The signals for Fe, C, O, S, and Si were clearly detected in the XPS spectrum (Fig. 2C) and EDX spectrum (Fig. 2F) of PVA-g-MNPs, confirming the successful immobilization of PVA onto MNPs surface by directly hydrolyzed of MNPs-PVAc and the successful growth of PVA onto MNPs surface by directly hydrolysis of MNPs-PVAc. Besides, we also observed that C1s peak with high intensity slightly shifted to a higher binding energy (BE) in the XPS of PVA-*g*-MNPs (Fig. 2C) which demonstrated that PVA polymeric chains were coated from the surfaces of MNPs.

Thermogravimetric simultaneous analysis was employed to determine the amount of precursor RAFT agents attached to MNPs (Fig. 3). Fig. 3A shows the TGA curve of MNPs. A weight loss of approximately 7.6 % was observed at temperatures below 300 ºC, which may be assigned to the weight loss of hydroxyl groups or absorbed gases on MNPs. As observed in TGA plot of MNPs-RAFT (Fig. 3B), the weight loss approximately 15.4 % between 50 and 800 ºC, corresponding to 7.8 % for the decomposition of the coupling RAFT agent phase onto MNPs. Thermogravimetric simultaneous analysis was used to determine the amount of PVA grafting from MNPs, which evaluated the thermal profile of organic and inorganic phase of PVA and MNPs (Fig. 3C). There are two weight loss steps was observed in Fig. 3C: (a) the initial step from 100 to 350 ºC may be assigned to the volatilization and decomposition of free and bound hydroxyl groups and; (b) the main thermal event took pace between 350 and 800 ºC would be due to the degradation of residual organic phases. Fig. 3D shows the TGA plot of PVA at the temperature range 50-800 ºC. The PVA shows a weight loss near to 25 % at $T_d$ of 284 ºC which is different from PVA-*g*-MNPs lost the same weight at $T_d$ of 336 ºC. This enhancement could explain that the nanocomposites exhibited the higher heat resistance imparted by the MNPs.

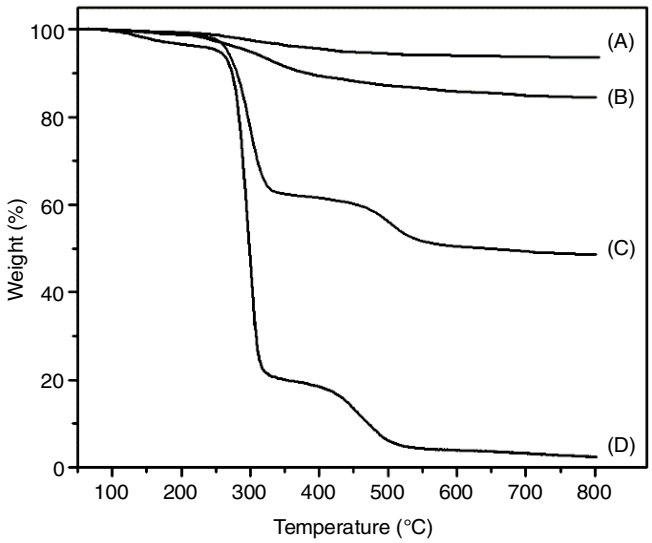


Fig. 3. TGA curves of (A) MNPs, (B) MNPs-RAFT, (C) PVA-g-MNPs and (D) polymer PVA

The room temperature magnetization curves of MNPs, MNPs-RAFT and PVA-g-MNPs obtained by VSM technique are shown in Fig. 4. There is no hysteresis curve in all samples, implying the characteristic super-paramagnetic behaviour of all the nanoparticles. The saturation magnetization values were determined to follow the order: MNPs (61.4 emu/g) > MNPs-RAFT (58.7 emu/g) > PVA-*g*-MNPs (35.8 emu/g). Compared with MNPs, MNPs-RAFT shows a little-decreased magnetization is due to MNPs content in these two samples was similar. The saturation magnetization of PVA-*g*-MNPs is significantly lower when compared with MNPs and MNPs-RAFT, which can be explained by the increase of the surface spins disorientation because the adsorbed polymer on the surface of MNPs changes the surface magnetic anisotropy. However, the observed level of saturation magnetization of PVA-*g*-MNPs is advantageous for biological applications.

**Drug loading/release properties and *in vitro* cytotoxicity assay of ibuprofen-load PVA coated MNPs:** Poly(vinyl aclcohol) presents good bioactivity, biocompatibility, non-toxic properties and hydroxyl groups, making it an ideal candidate for drug delivery systems of a variety of pharmaceutical molecules. Therefore, as expected, PVA-*g*-MNPs could be suitable for a carrier in drug release system. Ibuprofen is one of the most widely used non-steroidal analgesic and anti-inflammatory drugs has been extensively considered as a model drug for sustained and controlled drug delivery into PVA-*g*-MNPs. When ibuprofen is adsorbed on the surface carrier, OH groups on the surface carrier coordinate the carboxyl group of ibuprofen to form hydrogen bonds. The adsorption of ibuprofen on PVA-*g*-MNPs can confirm by FT-IR results (Fig. 1E). It is observed that while

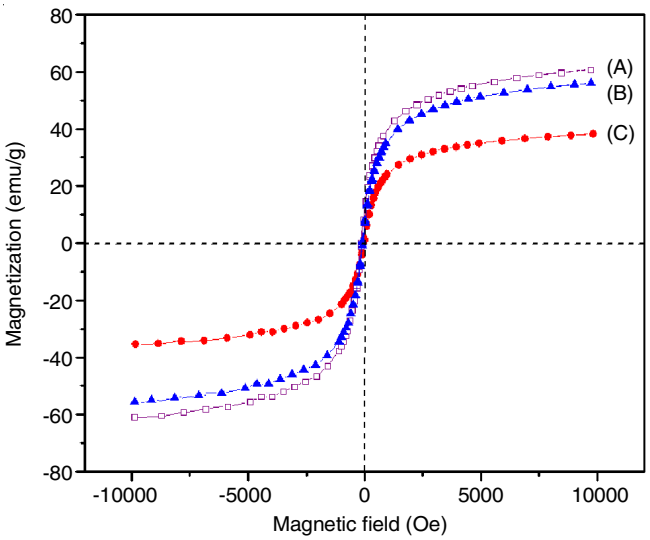


Fig. 4. Magnetization curves at 25°C for (A) MNPs, (B) MNPs-RAFT, and (C) PVA-g-MNPs

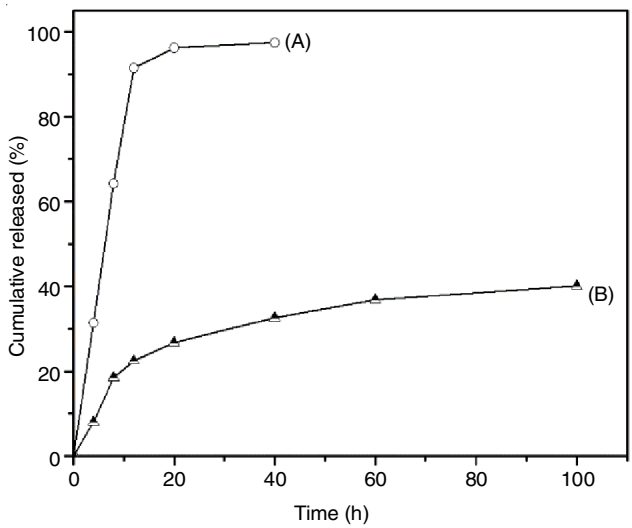


Fig. 5. *in vitro* IBU release curves of (A) pure IBU and (B) PVA-g-MNPs-IBU in SBF (pH = 7)

the band attributed to OH stretching (3380 $cm^{-1}$) was disappeared, the absorption peaks for carbonyl moiety (1723 $cm^{-1}$) and ether linkage (1613 $cm^{-1}$) originating from ibuprofen were appeared.

The cumulative drug release profiles for bare ibuprofen and ibuprofen loaded PVA-*g*-MNPs systems was examined as a function of release time in simulated body fluid (SBF). Fig. 5 plotted *in vitro* ibuprofen release curves of ibuprofen and PVA-*g*-MNPs-ibuprofen in SBF. The release rate of the bare ibuprofen in SBF was much faster than that of PVA-*g*-MNPs-ibuprofen system, which was completed within 10 h. By contrast, PVA-*g*-MNPs-ibuprofen exhibited a slow and sustained release of ibuprofen, about 26.7 % of loaded drug released in first 20 h and release rate reached at 40.1 % in 100 h. This result is advadageous for biological applications because it can avoid the explosive release of ibuprofen and prolong the drug effect. It is well known that ibuprofen release was determined by a diffusion process in the initial stage. In PVA-*g*-MNPs-ibuprofen system, due to the formation of hydrogen bonds between COOH groups of ibuprofen and OH groups of PVA grafted on MNPs, which slow or hold back the release of loaded ibuprofen. These results indicated that PVA-*g*-MNPs displayed much efficacy in controlling the initial burst release and achieving the sustained release as compared with bare ibuprofen.

To compare the cytotoxic effect of ibuprofen, PVA-*g*-MNPs and ibuprofen conjugates with PVA-*g*-MNPs, leading to inhibition of cell proliferation, standard MTT assay was performed on A549 and EA.hy926 cell lines (Fig. 6). As for the cytotoxicities of PVA-*g*-MNPs against the two cell lines, there is very little toxicity to the two cell lines and the cell viabilities of the two cell lines are still above 75 % at a high concentration (500 mg/ml). This result showed that PVA-*g*-MNPs is a tolerable carrier. As also seen in Fig. 6, the cell viabilities of two cell lines are below 40 % for both ibuprofen and PVA-*g*-MNPs-ibuprofen. It revealed that all the cancer cell lines exhibit a dose-dependent cytotoxicity for ibuprofen and PVA-*g*-MNPs-ibuprofen: higher dose of ibuprofen drugs correspond to greater cell inhibition. Conjugates of NSAIDs, including ibuprofen with nano-carrier, are frabicated in the hope of obtaining new forms of drug delivery systems that will address the potential relevance of their anticancer activity.

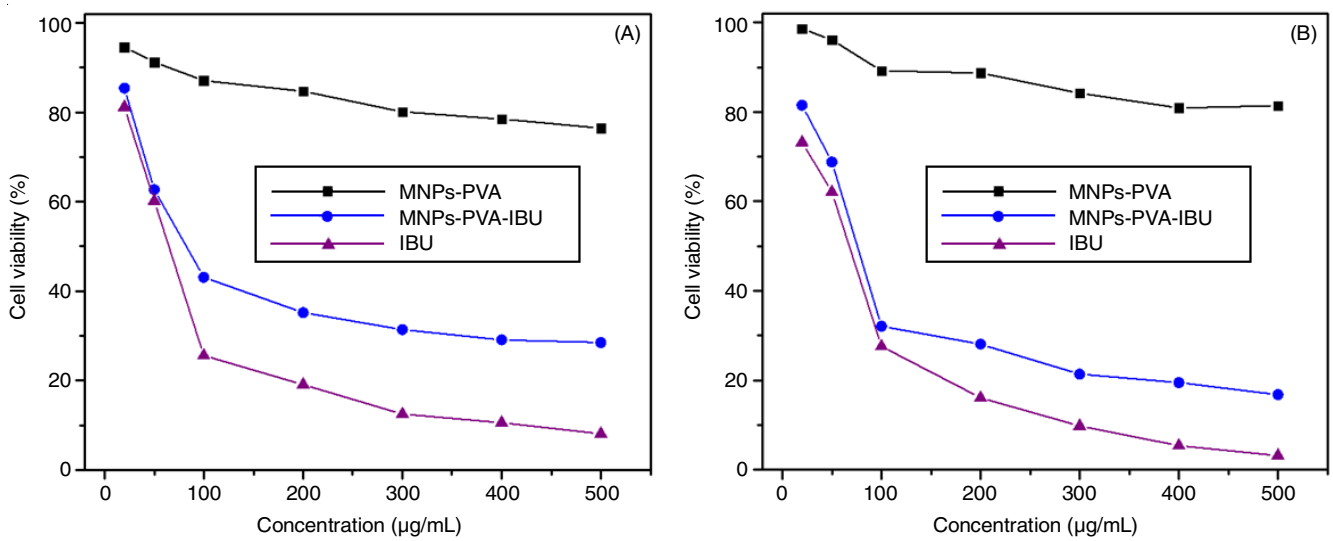


Fig. 6. Cell cytotoxicities of PVA-g-MNPs, PVA-g-MNPs-IBU and IBU PVA-g-MNPs against (A) A549 cells and (B) EA.hy926 at 48 h

## Conclusion

PVA-*g*-MNPs were succesfully prepared by RAFT polymerization. The chain transfer agent for RAFT was first immobilized onto the surface of MNPs. Subsequently, PVAc was grafted onto the MNPs surface through RAFT polymerization and then its hydrolysis. The PVA coated NMPs was unequivocally confirmed by FT-IR, XPS, EDS, TEM and TGA analyses. The magnetization curves of PVA-g-MNPs showed zero coercivity and remanence, displaying their super-paramagnetic property. Accordingly, an *in vitro* study on ibuprofen loading/releasing properties of magnetic carriers PVA-g-MNPs in SBF proposed a controlled release profile of ibuprofen from PVA-*g*-MNPs matrix which sustained for 62 h without obvious initial burst release. *In vitro* studies of the synthesized PVA-*g*-MNPs-ibuprofen nano-medicine suggested their promising activity against A549 cells and EA. Hy926. This approach may be generalized the development of smart materials based on MNPs with surface super-paramagnetic and hydrophilic properties, and therefore may serve as potential candidate for magnetically targeted drug delivery.

## ACKNOWLEDGEMENTS

This research is funded by Vietnam National Foundation for Science and Technology Development (NAFOSTED) under grant number 104.02-2014.53.

## REFERENCES

1. P. Aggarwal, J.B. Hall, C.B. McLeland, M.A. Dobrovolskaia and S.E. McNeil, *Adv. Drug Deliv. Rev.*, **61**, 428 (2009); https://doi.org/10.1016/j.addr.2009.03.009.
2. L.G. Bach, M. Rafiqul Islam, T.-S. Vo, S.-K. Kim and K.T. Lim, *J. Colloid Interface Sci.*, **394**, 132 (2013); https://doi.org/10.1016/j.jcis.2012.11.068.
3. J. Rivas, M. Bañobre-López, Y. Piñeiro-Redondo, B. Rivas and M.A. López-Quintela, *J. Magn. Magn. Mater.*, **324**, 3499 (2012); https://doi.org/10.1016/j.jmmm.2012.02.075.
4. J.K. Oh and J.M. Park, *Prog. Polym. Sci.*, **36**, 168 (2011); https://doi.org/10.1016/j.progpolymsci.2010.08.005.
5. L. Stanciu, Y.-H. Won, M. Ganesana and S. Andreescu, *Sensors*, **9**, 2976 (2009); https://doi.org/10.3390/s90402976.
6. J. Gao, H. Gu and B. Xu, *Acc. Chem. Res.*, **42**, 1097 (2009); https://doi.org/10.1021/ar9000026.
7. E. Cheraghipour, A.M. Tamaddon, S. Javadpour and I.J. Bruce, *J. Magn. Magn. Mater.*, **328**, 91 (2013); https://doi.org/10.1016/j.jmmm.2012.09.042.
8. S. Qin, L. Wang, X. Zhang and G. Su, *Appl. Surf. Sci.*, **257**, 731 (2010); https://doi.org/10.1016/j.apsusc.2010.07.050.
9. W. Brullot, N.K. Reddy, J. Wouters, V.K. Valev, B. Goderis, J. Vermant and T. Verbiest, *J. Magn. Magn. Mater.*, **324**, 1919 (2012); https://doi.org/10.1016/j.jmmm.2012.01.032.
10. M.R. Islam, L.G. Bach, S.Y. Seo and K.T. Lim, *J. Nanosci. Nanotechnol.*, **13**, 603 (2013); https://doi.org/10.1166/jnn.2013.6926.
11. S. Laurent, D. Forge, M. Port, A. Roch, C. Robic, L. Vander Elst and R.N. Muller, *Chem. Rev.*, **108**, 2064 (2008); https://doi.org/10.1021/cr068445e.
12. U. Westedt, M. Kalinowski, M. Wittmar, T. Merdan, F. Unger, J. Fuchs, S. Schäller, U. Bakowsky and T. Kissel, *J. Control. Rel.*, **119**, 41 (2007); https://doi.org/10.1016/j.jconrel.2007.01.009.
13. Y.-Y. Tong, Y.-Q. Dong, F.-S. Du and Z.-C. Li, *J. Polym. Sci. A Polym. Chem.*, **47**, 1901 (2009); https://doi.org/10.1002/pola.23288.
14. S.B.-D. Makhluf, R. Abu-Mukh, S. Rubinstein, H. Breitbart and A. Gedanken, *Small*, **4**, 1453 (2008); https://doi.org/10.1002/smll.200701308.
15. S. Kayal and R.V. Ramanujan, *Mater. Sci. Eng. C*, **30**, 484 (2010); https://doi.org/10.1016/j.msec.2010.01.006.
16. A.K. Bajpai and R. Gupta, *J. Mater. Sci. Mater. Med.*, **22**, 357 (2011); https://doi.org/10.1007/s10856-010-4214-2.
17. P.H.C. Camargo, K.G. Satyanarayana and F. Wypych, *Mater. Res.*, **12**, 1 (2009); https://doi.org/10.1590/S1516-14392009000100002.
18. R. Barbey, L. Lavanant, D. Paripovic, N. Schüwer, C. Sugnaux, S. Tugulu and H.-A. Klok, *Chem. Rev.*, **109**, 5437 (2009); https://doi.org/10.1021/cr900045a.
19. M.C. Daniel and D. Astruc, *Chem. Rev.*, **104**, 293 (2004); https://doi.org/10.1021/cr030698+.
20. M. Beija, J.-D. Marty and M. Destarac, *Prog. Polym. Sci.*, **36**, 845 (2011); https://doi.org/10.1016/j.progpolymsci.2011.01.002.
21. D.J. Keddie, G. Moad, E. Rizzardo and S.H. Thang, *Macromolecules*, **45**, 5321 (2012); https://doi.org/10.1021/ma300410v.
22. C. Boyer, M.H. Stenzel and T.P. Davis, *J. Polym. Sci. A Polym. Chem.*, **49**, 551 (2011); https://doi.org/10.1002/pola.24482.
23. V.G. Ngo, C. Bressy, C. Leroux and A. Margaillan, *Polymer*, **50**, 3095 (2009); https://doi.org/10.1016/j.polymer.2009.04.077.
24. Z.-P. Xiao, K.-M. Yang, H. Liang and J. Lu, *J. Polym. Sci. A Polym. Chem.*, **48**, 542 (2010); https://doi.org/10.1002/pola.23752.
25. J.S. van Leeuwen, B. Ünlü, N.P.E. Vermeulen and J.C. Vos, *Toxicol. Vitr.*, **26**, 197 (2012); https://doi.org/10.1016/j.tiv.2011.11.013.
26. L. Bédouet, F. Pascale, M. Bonneau, M. Wassef and A. Laurent, *Toxicol. Vitr.*, **25**, 1944 (2011); https://doi.org/10.1016/j.tiv.2011.06.018.
27. M.L. Carty, J.A. Wixey, H.E. Reinebrant, G. Gobe, P.B. Colditz and K.M. Buller, *Brain Res.*, **1402**, 9 (2011); https://doi.org/10.1016/j.brainres.2011.06.001.
28. M. Sasidharan, H.N. Luitel, N. Gunawardhana, M. Inoue, S. Yusa, T. Watari and K. Nakashima, *Mater. Lett.*, **73**, 4 (2012); https://doi.org/10.1016/j.matlet.2011.12.058.
29. F. Chen, P. Huang, Y.-J. Zhu, J. Wu and D.-X. Cui, *Biomaterials*, **33**, 6447 (2012); https://doi.org/10.1016/j.biomaterials.2012.05.059.
30. L. Wang, R. Liao and X. Li, *Powder Technol.*, **235**, 103 (2013); https://doi.org/10.1016/j.powtec.2012.10.001.
31. Z. Xu, B. Li, W. Tang, T. Chen, H. Zhang and Q. Wang, *Colloids Surf. B Biointerfaces*, **88**, 51 (2011); https://doi.org/10.1016/j.colsurfb.2011.05.055.
32. T. Liu, Y. Wang, H. Qin, X. Bai, B. Dong, L. Sun and H. Song, *Mater. Res. Bull.*, **46**, 2296 (2011); https://doi.org/10.1016/j.materresbull.2011.08.056.
33. Y. Zhao and S. Perrier, *Macromolecules*, **40**, 9116 (2007); https://doi.org/10.1021/ma0716783.
34. T. Kokubo and H. Takadama, *Biomaterials*, **27**, 2907 (2006); https://doi.org/10.1016/j.biomaterials.2006.01.017.